ACS APPLIED MATERIALS & INTERFACES

Research Article

www.acsami.org

Fabrication of Propeller-Shaped Supra-amphiphile for Construction of Enzyme-Responsive Fluorescent Vesicles

Jie Li,[†] Kaerdun Liu,[†] Yuchun Han,[‡] Ben Zhong Tang,*[,§] Jianbin Huang,*[,†] and Yun Yan*[,†]

[†]Beijing National Laboratory for Molecular Sciences (BNLMS), College of Chemistry and Molecular Engineering, Peking University, Beijing 100871, China

[‡]Institute of Chemistry, Chinese Academy of Sciences, Beijing, China

[§]Department of Chemistry, Hong Kong Branch of Chinese National Engineering Research Center for Tissue Restoration & Reconstruction, The Hong Kong University of Science & Technology, Clear Water Bay, Kowloon, Hong Kong, China

Supporting Information

ABSTRACT: Propeller-shaped molecules have been recognized to display fantastic AIE (aggregation induced emission), but they can hardly self-assemble into nanostructures. Herein, we for the first time report that ionic complexation between a water-soluble tetrapheneyl derivative and an enzyme substrate in aqueous media produces a propeller-shaped supra-amphiphile that self-assembles into enzyme responsive fluorescent vesicles. The supra-amphiphile was fabricated upon complexation between a water-soluble propeller-shaped AIE luminogen TPE-BPA and myristoylcholine chloride (MChCl) in aqueous media. MChCl filled in the intramolecular voids of propeller-shaped TPE-BPA upon supra-amphiphile formation, which endows the supra-amphiphile superior self-assembling ability to the component molecules thus leading to the formation of fluorescent vesicles. Because MChCl is the substrate of cholinesterases, the vesicles dissemble in the presence of cholinesterases, and the fluorescent intensity can be correlated to the level of enzymes. The resulting fluorescent vesicles may be used to recognize the site of Alzheimer's disease, to encapsulate the enzyme inhibitor, and to release the inhibitor at the disease site.

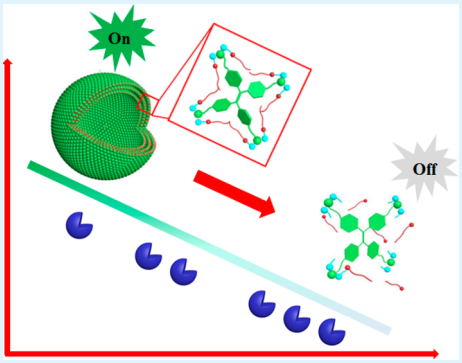

KEYWORDS: *enzyme-responsive, AIE, fluorescent vesicle, self-assembly, supra-amphiphile*

INTRODUCTION

Supramolecular building blocks, or supra-amphiphiles, have recently attracted intensive interest in the field of molecular self-assembly because they allow facile fabrication of the topological molecular unit leading to judicious functional self-assembled structures.[1−4] Different from normal covalent ones, supra-amphiphiles are formed on the basis of noncovalent interactions between two molecular building blocks via $\pi-\pi$ interaction, hydrogen bonding, charge-transfer interaction, electrostatic interaction, host−guest interaction, etc.[5] The distinct advantage of supra-amphiphiles is the facile combination of functional groups under mild condition. This not only avoids tedious and time-consuming chemical syntheses, but also allows employment of biomolecules to construct nanoscaled vectors for disease relating applications. Furthermore, stimuli-responsive functional moieties can be easily introduced into supra-amphiphiles via noncovalent interactions, it is possible to control the self-assembling and disassembling process of the nanostructures. The excellent work by Lehn,[6,7] Zhang,[8−10] Liu,[11] Schmuck,[12] Huang,[13−15] Yan,[16] and others[17−22] have demonstrated that supra-amphiphiles often endows superior self-assembling ability to their component molecular building blocks, thus not only enrich the family of normal covalent amphiphiles but also provide a new connection between nature and the supramolecular sciences.

As a new class of dyes that displaying aggregation-induced emission (AIE),[23] nonconjugated propeller-shaped molecules was found very appealing in a number of fields, such as organic light-emitting materials,[24,25] chemical sensors,[26,27] and bioprobes and bioimaging agent.[28−33] Different from conventional planar dyes that always undergo $\pi-\pi$ stacking which results in notorious aggregation-caused quenching (ACQ),[34] the propeller-shaped AIE dyes are nonplanar so that they usually do not stack even in solid state thus give out intensive emission.[35] However, the biggest drawback of the propeller-shaped topology is that it disfavors self-assembly, so that fluorescent nanostructures based on AIE molecules are still very rarely up to date. To tackle this issue, tremendous covalent modification has been adopted to endow the AIE dyes self-assembling ability.[36−41] Herein, we use a simple and straightforward supra-amphiphile method for production of fluorescent vesicles based on propeller-shaped AIE dye. We show in this work that the AIE dye TPE-BPA can form extremely stable TPE-BPA@

Received: July 15, 2016
Accepted: September 26, 2016
Published: September 26, 2016

DOI: 10.1021/acsami.6b08620
ACS Appl. Mater. Interfaces 2016, 8, 27987−27995

Scheme 1. Schematic Illustration of the Self-Assembly and Disassembly Processes of Fluorescent Vesicles Caused by Enzyme AChE: (a) Structures of TPE-BPA and MChCl, (b) Enzymolytic Reaction of MChCl and (c) Self-Assembly and Disassembly Processes of Fluorescence Vesicle

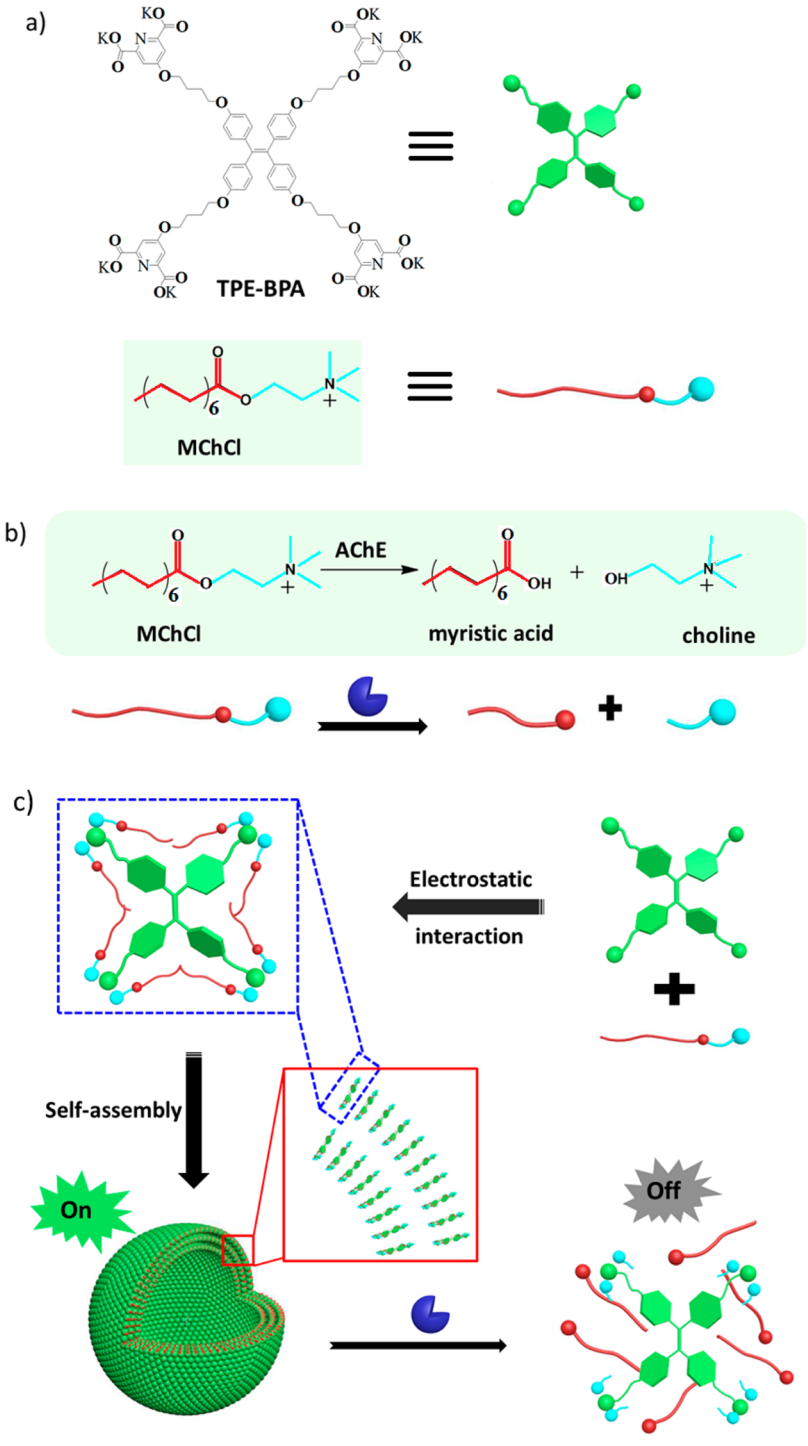

8MChCl supra-amphiphile with myristoylcholine chloride (MChCl) via ionic interaction. Although the TPE-BPA@8MChCl supra-amphiphile inherits the propeller-shaped topology of TPE-BPA, it has strong self-assembling ability and can facilely self-assemble into fluorescent vesicles around 110 nm via hydrophobic effect. Because MChCl is the substrate of cholinesterase,[42] the vesicular structure can be disassembled by cholinesterase, which simultaneously triggers the loss of fluorescence. Significantly, the fluorescence intensity can be correlated to the level of cholinesterase, which is overexpressed in the Alzheimer's disease.[43−46] Thus, this work reveals that fabrication of supramolecular building block not only endows self-assembling ability to the propeller-shaped AIE molecule, but also opens up the avenue toward facile fabrication of medically relevant nanostructures. Specifically, the enzyme-responsive fluorescent vesicle is expected to generate a novel family of luminescent nanocarriers with combined abilities of image-guiding, target-releasing, and therapy tracking.

DOI: 10.1021/acsami.6b08620
ACS Appl. Mater. Interfaces 2016, 8, 27987−27995

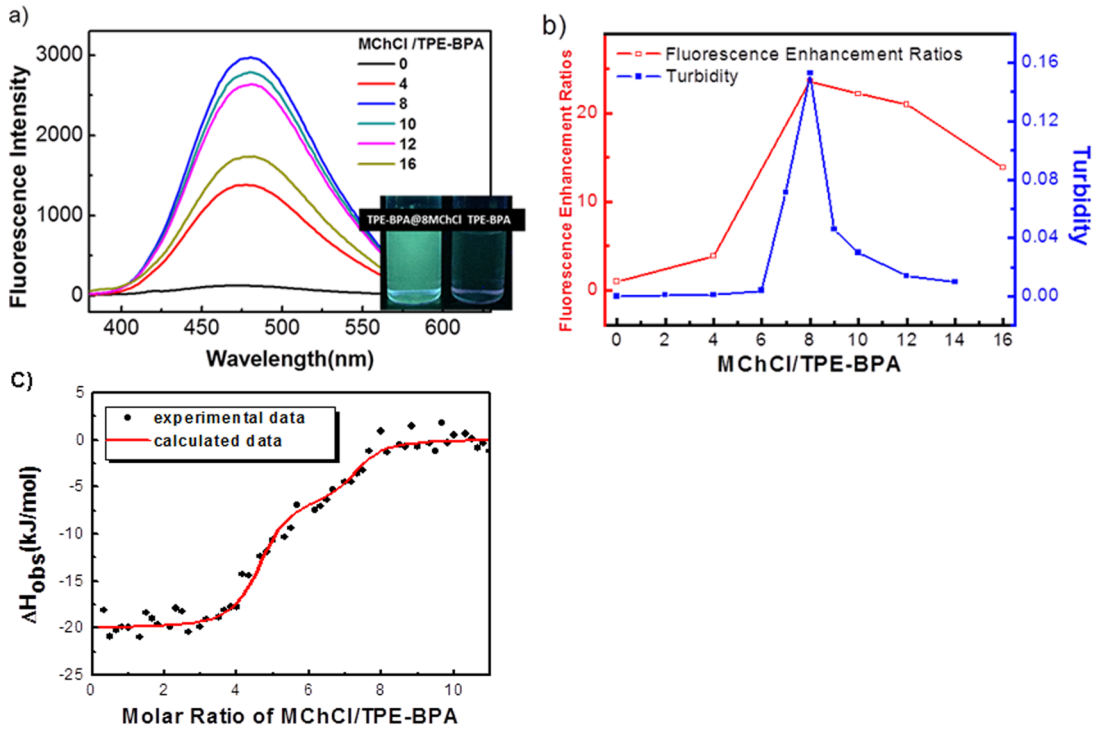

Figure 1. (a) Fluorescence spectra of TPE-BPA at different MChCl/TPE-BPA molar ratios. Inset: the photos of aqueous solution of TPE-BPA and that of TPE-BPA@8MChCl under UV irradiation (λ_{ex} = 365 nm). (b) The variation in the solution turbidity (blue, λ = 600 nm) and fluorescence enhancement ratios (FER) at different ratios of MChCl/TPE-BPA. The FER were obtained by normalizing the fluorescence intensity in the MChCl/TPE-BPA systems with respect to that of the MChCl free system. (c) ITC titration curves for the MChCl/TPE-BPA system. All the measurements were performed at 25 °C, the concentration of TPE-BPA was kept at 0.05 mM, and the excitation wavelength (λ_{ex}) is set at 365 nm.

RESULTS AND DISCUSSION

Formation of Ionic Supra-amphiphile TPE-BPA@8MChCl. TPE-BPA was obtained by endowing the typical AIE group tetraphenylethylene (TPE)[47−50] with four water-soluble hydrophilic carboxylate heads (Scheme 1a). TPE-BPA can hardly aggregate in water which is characterized by the weak fluorescence. However, the fluorescence was drastically enhanced as the oppositely charged myristoylcholine chloride (MChCl) was added (Figure 1a), and the maximum enhancement occurs at the molar ratio of MChCl/TPE-BPA = 8 (Figure 1b). Because each TPE-BPA carries 8 elementary negative charges, whereas each MChCl carries only 1 positive charge, it is obvious that strong electrostatic interaction has occurred. In the meanwhile, isothermal titration calorimetry (ITC) measurements indicated the occurrence of two-step complexation between TPE-BPA and MChCl, corresponding to two binding ratios of MChCl:TPE-BPA being 5:1 and 3:1, respectively. This gives an overall binding ratio of 8:1, suggesting the formation of the supramolecular building block of TPE-BPA@8MChCl. It is very striking that the binding constants associated with the two steps are 2.87×10^7 M^{-1} and 4.08×10^5 M^{-1}, which are 1×10^4 and 1×10^2 times higher than the host−guest binding constants between cyclodextrin and surfactant,[51] respectively, indicating the ionic supra-amphiphile TPE-BPA@8MChCl is very stable.

Self-Assembly of TPE-BPA@8MChCl Supra-amphiphile into Fluorescent Vesicles. The TPE-BPA@8MChCl supra-amphiphile can further self-assemble into colloidal particles which are accompanied by the maximum fluorescence and the strongest turbidity (Figure 1b). Dynamic light scattering (DLS) measurement showed the particles have a narrow size distribution with an average hydrodynamic radius (R_h) around 110 nm (Figure 2a). Cryo-TEM observation revealed the formation of vesicles with radius ranging from 100−200 nm (Figure 2b). Confocal laser scanning microscopy

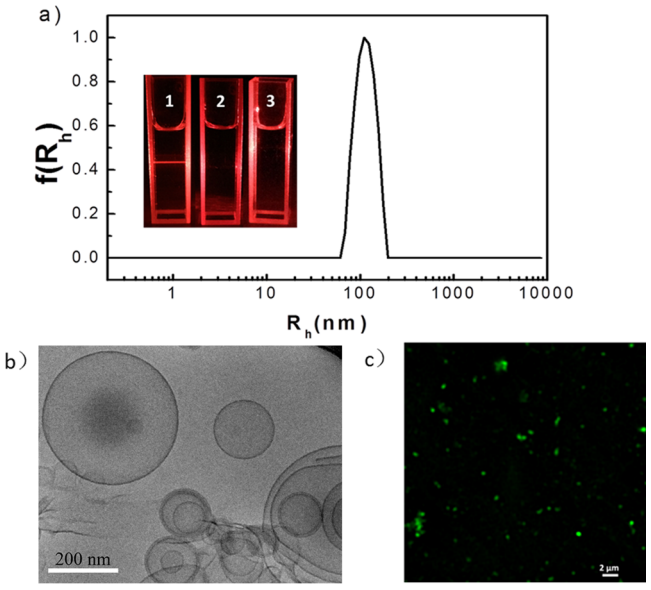

Figure 2. (a) DLS size distribution, (b) cryo-TEM image, and (c) CLSM image for the vesicles formed in the TPE-BPA@8MChCl system. [TPE-BPA] = 0.05 mM, [MChCl] = 0.40 mM. The inset in a shows the photos of light path under laser irradiation for the aqueous system of (1) TPE-BPA@8MChCl, (2) TPE-BPA, and (3) MChCl, respectively.

DOI: 10.1021/acsami.6b08620
ACS Appl. Mater. Interfaces 2016, 8, 27987−27995

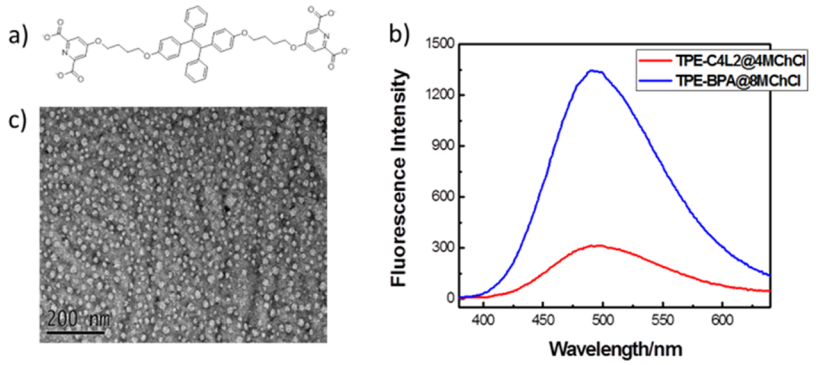

Figure 3. (a) Structure of TPE-C4-L2, (b) fluorescence spectra of TPE-BPA@8MChCl and TPE-C4-L2@4MChCl. (C) TEM image of TPE-C4-L2@4MChCl. [TPE-BPA] = [TPE-C4-L2] = 0.05 mM.

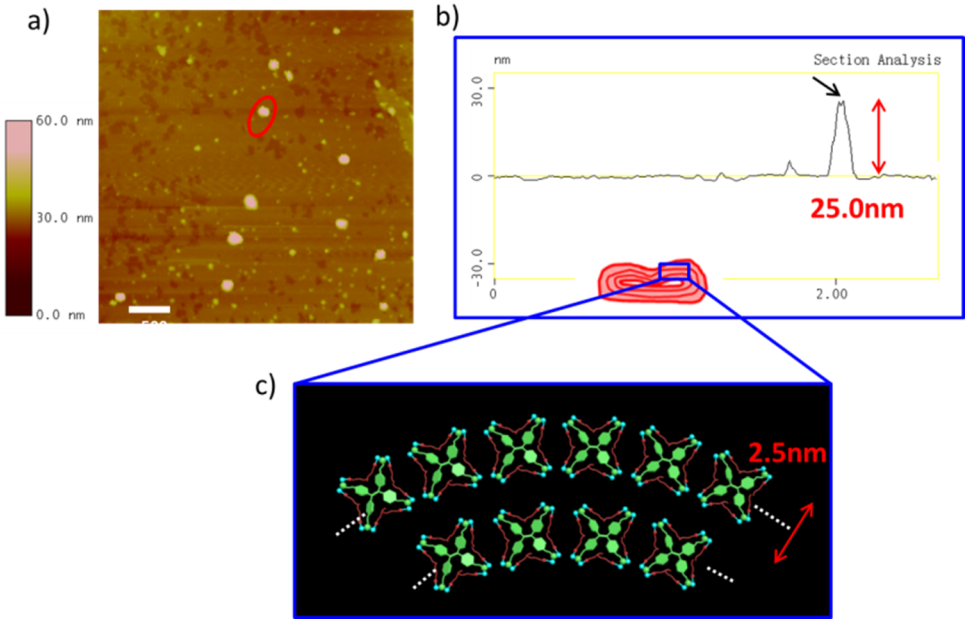

Figure 4. (a) AFM image of the vesicles formed in the TPE-BPA@8MChCl system. (b) Height profile of the circled vesicle membrane in a. (c) Illustration of the molecular arrangement in the collapsed vesicle membrane. [TPE-BPA] = 0.05 mM, [MChCl] = 0.40 mM.

(CLSM) observations (Figure 2c) clearly revealed the green fluorescence for these vesicles.

To further understand the supramolecular details of TPE-BPA@8MChCl, we performed NOSY NMR measurements. Figure S1 reveals there is no correlation for the protons in TPE-BPA and MChCl, indicating that the hydrocarbon portion of these two molecules are not contacting with each other. This means that MChCl has filled in the gaps of the propeller-shaped TPE-BPA molecules (Scheme 1a). It is possible that such molecular arrangement efficiently increases the hydrophobic effect despite of the propeller-shaped topology so that the self-assembling ability is enhanced.

It is noted that the charge density of TPE-BPA plays a significant role on self-assembly of vesicles. When the charge of TPE-BPA decreases to 4 (TPE-C4-L2), compared with TPE-BPA@8MChCl, the fluorescence emission is extremely weak. TEM observation reveals that only small clusters were formed (Figure 3), suggesting that the compact packing of hydrocarbon chains in the TPE-BPA@8MChCl supramolecule endows a much stronger AIE effect.

Because TPE-BPA can be viewed as a bola-amphiphile[52−55] that forms a monolayer vesicle membrane rather than those bilayer ones as classical lipids,[56] the membrane thickness of the vesicles should be only formulated by the TPE-BPA molecule, whereas the MChCl, with an extending length of 2.0 nm, imbeds in the TPE-BPA voids. The atomic force microscope (AFM) image in Figure 4 revealed that the thickness (height) of one collapsed vesicle is about 25 nm, which is 10 times of the extending length of one TPE-BPA. The indicated vesicle is expected to have 5 shells. There are also vesicles with 6 and 7 shells (Figure S2), suggesting the vesicles are predominantly multilayered, as illustrated in Figure 4.

These multilayered TPE-BPA@8MChCl vesicles possess high stability against ionic screening (Figure S3a), and can be kept in phosphate-buffered saline (PBS, pH 7.4) and without any change either in morphology or size for days (Figure S3b). This ultrahigh stability of the vesicles is in drastic contrast to self-assemblies driven solely via electrostatic interactions, suggesting hydrophobic effect between the TPE-BPA@8MChCl supra-amphiphiles is the main driving forces for the vesicle formation, whereas ionic interactions are mainly responsible for the formation of the supramolecular building blocks. Furthermore, DSC measurements suggests no melting of membrane in the temperature range of 20−90 °C (Figure

DOI: 10.1021/acsami.6b08620
ACS Appl. Mater. Interfaces 2016, 8, 27987−27995

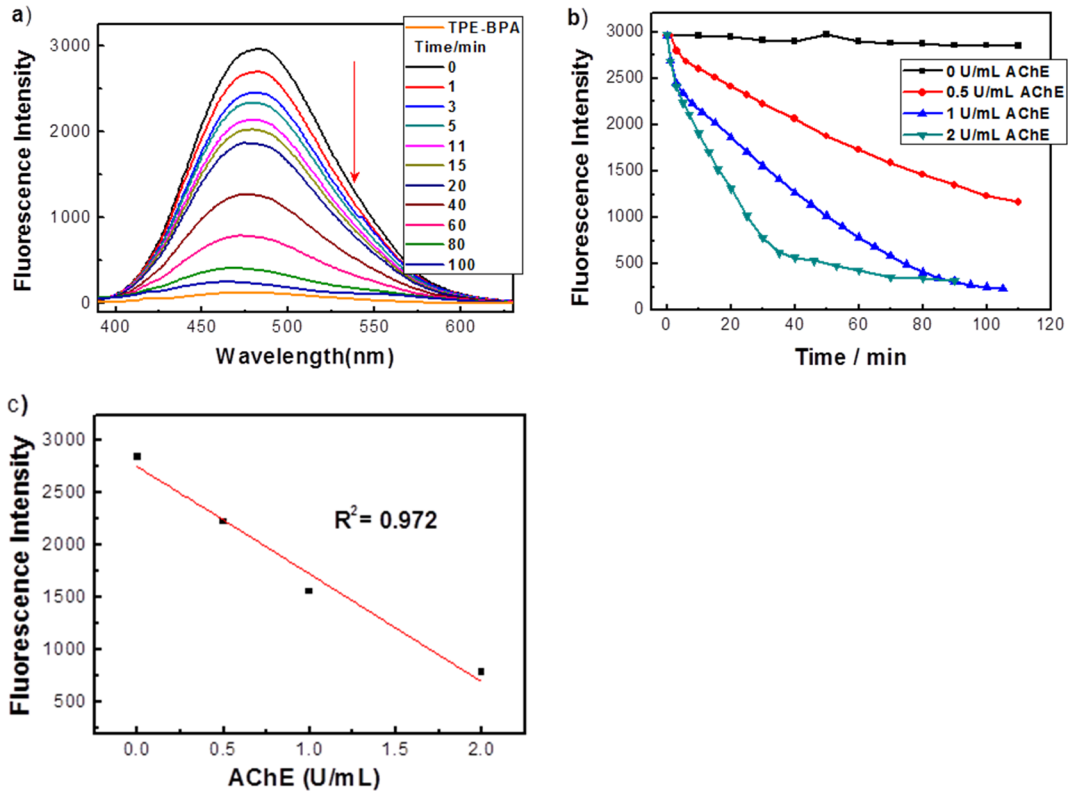

Figure 5. (a) Variation of the fluorescence in the TPE-BPA@8MChCl systems in the presence of 1 U/ml AChE over time. (b) Decay rates of the fluorescence in the TPE-BPA@8MChCl system as the concentration of AChE is 0, 0.5, 1, and 2 U/mL. (c) Plots of the fluorescence changes in the TPE-BPA@8MChCl systems at 480 nm after addition of different concentrations of AChE for 30 min. [TPE-BPA] = 0.05 mM, [MChCl] = 0.40 mM.

S4), indicating that the vesicles are very robust, which is comparable with polymeric vesicles.

Enzyme Response of Vesicle. The ultrahigh stability of the TPE-BPA@8MChCl vesicle allows further application of them as fluorescent drug carrier in biological environment. First of all, the empty TPE-BPA@8MChCl vesicle was subjected to acetylcholinesterase (AChE), since MChCl can be hydrolyzed by cholinesterase. AChE is a kind of cholinesterase in brain, the level of which is closely related with Alzheimer's disease.[57,58] Figure 5a shows that after addition of 1 U/mL AChE into the TPE-BPA@8MChCl solution, the fluorescence decreased rapidly to the level close to that of the free TPE-BPA, indicating the disassembly of the vesicles. The CLSM observations in Figure 6 displays the real time change of the fluorescent vesicles. At the beginning, the vesicles are regular fluorescent spheres in solution. Thirty min later, the spheres are fractured and became irregular, then transform into bar-like aggregates. Finally, hardly any vesicles can be observed after 1 day. The disruptive process is also confirmed by DLS and TEM (Figures S5 and S6). It should be noted that the TPE-BPA@8MChCl vesicle is only responsive to specific enzymes: the fluorescence intensities decrease can only be achieved with cholinesterases, such as AChE and BChE (butyrylcholinesterase), both are correlated to Alzheimer's' disease;[57,58] other enzymes, such as peroxidase and gluocose oxidase (GOx), have no effect on the fluorescence (Figure S7).

It is remarkable that the rate of fluorescence reduction depends on the concentrations of AChE (Figure 5b). The slope of the fluorescence reduction in the initial 20 min can be used to express the rate of the enzyme reaction. A linear reduction of the enzyme level with time is obtained in the AChE concentration range of 0−2 U/mL (Figure 5c), implying that the fluorescence intensity can be used to track the levels of cholinesterases.

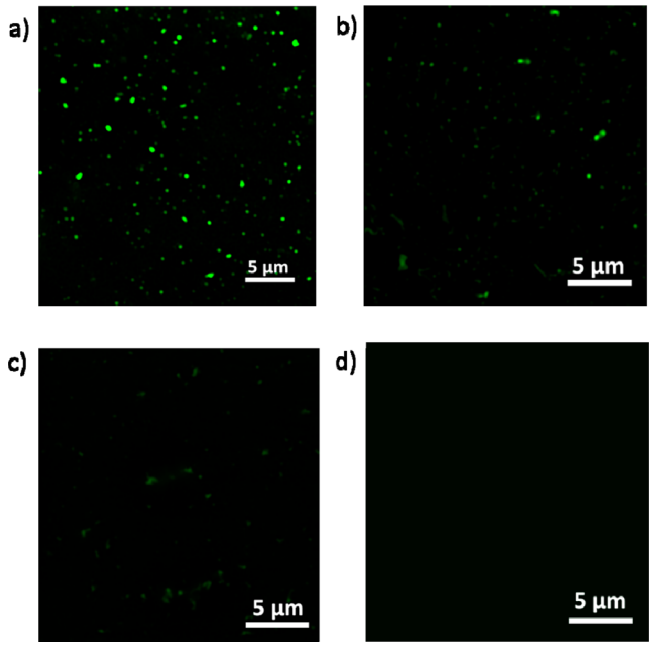

Figure 6. Real-time CLSM images of the TPE-BPA@8MChCl system in the presence of 1 U/mL AChE. (a) 0, (b) 1.5, (c) 3, and (d) 24 h. [TPE-BPA] = 0.05 mM, [MChCl] = 0.40 mM.

DOI: 10.1021/acsami.6b08620
ACS Appl. Mater. Interfaces 2016, 8, 27987−27995

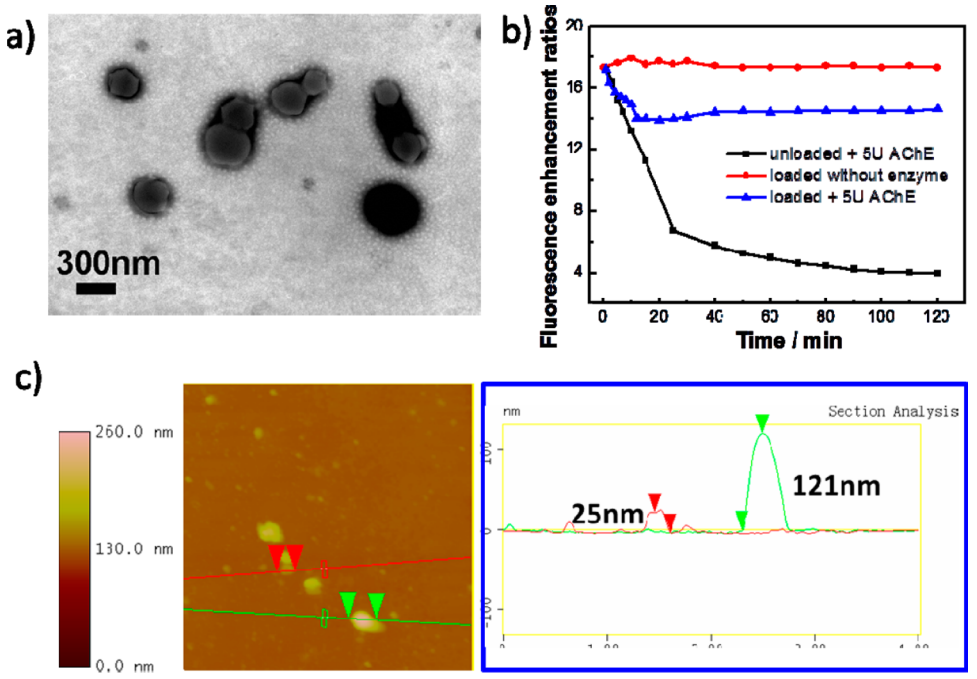

Figure 7. (a) TEM images of tacrine-loaded vesicles. (b) Change of fluorescence enhancement ratios (FER) of the vesicles in the presence of 5 U/mL AChE over time. (c) AFM image of tacrine-loaded vesicles. [TPE-BPA] = 0.05 mM, [MChCl] = 0.40 mM.

The rupture of the vesicles in the presence of AChE can be attributed to the hydrolyzing of the positively charged MChCl into myristic acid and small choline cation (Scheme 1b). Mass spectrum (MS) measurements indicate that the peak corresponding to $[MCh]^+$at M/Z = 314 (Figure S8) gradually reduced over time in the presence of AChE, whereas it kept almost constant when AChE is absent, signifying hydrolyzing of MChCl by enzyme AChE. The hydrolyzed products, although contain positively charged choline, can hardly form ion pairs with TPE-BPA due to its excellent solubility in water. The other component, myristic acid, which may carry negative charges upon partly dissociation, repels with TPE-BPA and cannot trigger the aggregation or self-assembly of TPE-BPA, as well. As a result, the vesicles have to disassemble (Scheme 1).

Drug Release. The decrease in fluorescence intensity accompanied by the rupture of vesicles offers a facile and convenient analytical approach to inspect the releasing status of loaded drugs. Tacrine, a typical water-soluble cholinesterase inhibitor for the clinical treatment of Alzheimer's disease, was loaded into the fluorescent vesicles. Note that the height of tacrine-loaded vesicle was about 120 nm (Figure 7a, c), which was much larger than the height of unloaded vesicles (25−30 nm, Figure 4a). Without AChE, the fluorescence intensity of tacrine-loaded vesicles did not change within 2 h (Figure 7b). This is in good agreement with the superior stability of the vesicles in biological environment (Figure S4). However, as the AChE was added, the fluorescence intensity of the loaded vesicles reduced by about 20%, which is in clear contrast with the drastic decrease of the fluorescence for the unloaded vesicles (Figure 7). This implies that the released drug have successfully inhibited the activity of the AChE, preventing the remained vesicles from further rupture (Scheme 2 and Figure S9). In this sense, this enzyme responsive fluorescent MChCl/TPE-BPA vesicle not only allows targeted delivery and smart releasing of drugs for Alzheimer's disease but also enables them to monitor the path of the drugs using the remained fluorescence, which facilitates the accurate diagnosis and real-time analysis of the therapeutic efficiency.

Scheme 2. Illustration of the Partial Disassembly of the Fluorescent Vesicles Loaded with Tacrines (pink spheres) by the Enzyme AChE[a]

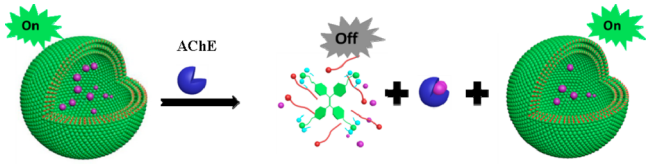

[a]Some of the vesicles were ruptured to release tacrines, and the released tacrines inhibit the activity of enzyme AChE to prevent the remaining vesicles from further rupture.

CONCLUSION

In summary, our study presents a new type of enzyme responsive fluorescent vesicle for the image-guiding, target-releasing, and therapy tracking for Alzheimer's disease. In this system, the fluorescent vesicles were formed by self-assemble the ionic supramolecular building block of TPE-BPA@8MChCl, where TPE-BPA is a propeller-shaped luminogen displaying aggregation induced emission, and MChCl (myristoylcholine chloride) is the substrate for cholinesterases. The obtained vesicle can only be broken by cholinesterases, which is accompanied by the decrease of the fluorescence intensity. Strikingly, the fluorescence of the vesicles is proportional to the enzyme level, thus can be used to report the therapeutic response. Because the cholinesterases are overexpressed in the Alzheimer's disease, such drug-loaded enzyme-responsive fluorescent vesicle combines the image-guiding, target-releasing, and therapy tracking functions in one nanocarrier, which may have great potential as a an effective nanodrug promising for therapy of Alzheimer's disease. Moreover, the supramolecular strategy of fabrication of fluorescent vesicles reported in this

DOI: 10.1021/acsami.6b08620
ACS Appl. Mater. Interfaces 2016, 8, 27987−27995

work may be extended to the other types of biomolecules of interests, to develop novel fluorescent vesicle-based nanodrugs with interesting functions and properties useful in biomedicine.

EXPERIMENTAL SECTION

Materials. TPE-BPA was synthesized according to the procedure in the Supporting Information. Myristoylcholine chloride (MChCl), tacrine, butyrylcholinesterase (BChE, from equine serum), and acetylcholinesterase (AChE, from *Electrophorus electricus*) were purchased from Sigma-Aldrich. The other reagents were of analytical reagent grade. Aqueous solutions were prepared using Milli-Q water of 18 MΩ.

Spectra Measurements. Turbidity measurements were carried out on the SHIMADZU UV-1800 spectrophotometer at 600 nm at room temperature (RT). Fluorescence spectra were recorded on a Hitachi F7000 spectrometer equipped with a constant temperature bath to control the temperature at 25 °C (λ_{ex} = 365 nm, bandwidth (ex) 2.5 nm, bandwidth (em) 5.0 nm).

Cryogenic Transmission Electronic Microscope (Cryo-TEM). A few microliters of samples were placed on a bare copper TEM grid (Plano, 600 mesh), and the excess liquid was removed with filter paper. This sample was cryo-fixed by rapidly immersing into liquid ethane cooled to −170 to −180 °C in a cryo-box (Carl Zeiss NTS GmbH). The specimen was inserted into a cryo-transfer holder (CT3500, Gatan, Munich, Germany) and transferred to a Zeiss EM922 EFTEM (Zeiss NTS GmbH, Oberkochen, Germany). Examinations were carried out at temperatures around −180 °C. The TEM was operated at an acceleration voltage of 200 kV. Zero-loss filtered images were taken under reduced dose conditions (500−2000 e/nm^2). All images were recorded digitally by a bottom-mounted CCD camera system (UltraScan 1000, Gatan) and processed with a digital imaging processing system (Digital Micrograph 3.9 for GMS 1.4, Gatan).

Transmission Electron Microscopy (TEM). TEM images were recorded on a JEM-100 CX II transmission electron microscope (JEOL, Japan, 80 kV). The samples were prepared by dropping solutions onto copper grids coated with Formvar film. Excess water was removed by filter paper, and the samples were stained with uranyl acetate and dried in ambient environment at room temperature for TEM observation.

Atomic Force Microscopy (AFM). AFM measurements were conducted on a VEECO D3100 AFM with a tapping mode under ambient conditions. One drop of the solution was spin-coated on silicon surface, and then dried at room temperature for AFM observation.

Isothermal Titration Calorimetry measurements (ITC). All measurements were performed in a TAM 2277−201 microcalorimetric system (Thermometric AB, Järfalla, Sweden) with a stainless steel sample cell of 1 mL. The sample cell was initially loaded with 0.7 mL of solvent or surfactant solution. The b-CD solution was injected into the sample cell via a 500 mL Hamilton syringe controlled by a 612 Thermometric Lund pump. A series of injections were made until the desired concentration range had been covered. The system was stirred at 60 rpm with a gold propeller. The observed enthalpy (DHobs) was obtained by integration over the peak for each injection in the plot of heat flow P against time t. The dilution heats of the b-CD solution were subtracted from the heats of the binding experiments. The data fitting was performed by using the computer program for TAM (Digitam 4.1 for Windows from Thermometric AB). By fitting the observed enthalpy curves plotted against the molar ratio of b-CD to surfactant, the binding stoichiometry *n*, binding constant (K) and the binding enthalpy (DH) were derived. All of the measurements were conducted at 298.15 ± 0.01 K.

Dynamic Light Scattering (DLS). DLS data were obtained on a laser light scattering spectrometer ALV/DLS/SLS5022F with a 22 mW He−Ne laser (λ= 632.8 nm) at room temperature. The scattering angle was 90°, and the intensity autocorrelation functions were analyzed by using the method of CONTIN. The mean apparent hydrodynamic radius (R_h) was obtained by

$$R_h = kTq^2/6\pi\eta\Gamma \quad (1)$$

where q is the scattering vector, k is the Boltzmann constant, T is the absolute temperature, η is the viscosity of the solvent, and Γ is the measured average decay rate of the correlation function.

Confocal Laser Scanning Microscopy (CLSM). The samples were observed directly without any staining. A drop of MChCl/TPE-BPA solution was sealed between two slides at room temperature and ready for CLSM observation. The CLSM experiments were conducted in florescence modes on N-SIM Confocal Laser Scanning Microscopy.

Tacrine Loading. A certain amount of TPE-BPA (5 mM), MChCl (5 mM), and tacrine (5 mM) were added into pH 7.4 PBS solutions until the volume reached 3 mL, where the concentrations of TPE-BPA, MChCl and tacrine were 50, 400, and 50 μM, respectively. Then, excess tacrines outside the vesicles were removed by dialysis (molecular weight cutoff 1000) in distilled water at 25 °C several times until the solutions outside the dialysis exhibited negligible tacrine UV signals.

ASSOCIATED CONTENT

Supporting Information

This material is available free of charge at The Supporting Information is available free of charge on the ACS Publications website at DOI: 10.1021/acsami.6b08620.

Additional experimental details for synthesis path of TPE-BPA, ITC, AFM, fluorescence Spectrum, DLS, SLS, DSC, TEM, and MS (PDF)

AUTHOR INFORMATION

Corresponding Authors

*E-mail: yunyan@pku.edu.cn.
*E-mail: jbhuang@pku.edu.cn.
*E-mail: tangbenz@ust.hk.

Notes

The authors declare no competing financial interest.

ACKNOWLEDGMENTS

This work is supported by the National Science Foundation of China (NSFC, Grant No. 21422302, 21573011), National Basic Research Program of China (2013CB933800), and "the Innovation and Technology Commission of Hong Kong (ITC-CNERC14S01)".

REFERENCES

(1) Ariga, K.; Lvov, Y.; Kunitake, T. Assembling Alternate Dye−Polyion Molecular Films by Electrostatic Layer-by-Layer Adsorption. *J. Am. Chem. Soc.* **1997**, *119*, 2224−2231.

(2) Wang, A.; Huang, J.; Yan, Y. Hierarchical molecular self-assemblies: construction and advantages. *Soft Matter* **2014**, *10*, 3362−3373.

(3) Chakrabarty, R.; Mukherjee, P. S.; Stang, P. J. Supramolecular Coordination: Self-Assembly of Finite Two- and Three-Dimensional Ensembles. *Chem. Rev.* **2011**, *111*, 6810−6918.

(4) Wang, A. D.; Huang, J. B.; Yan, Y. Hierarchical molecular self-assemblies: construction and advantages. *Soft Matter* **2014**, *10*, 3362−3373.

(5) Kang, Y. T.; Liu, K.; Zhang, X. Supra-Amphiphiles: A New Bridge Between Colloidal Science and Supramolecular Chemistry. *Langmuir* **2014**, *30*, 5989−6001.

(6) Jullien, L.; Lazrak, T.; Canceill, J.; Lacombe, L.; Lehn, J. M. An Approach to Channel-Type Molecular-Structures 0.3. Incorporation Studies of the Bouquet-Shaped B(M) and B(Cd) in Phosphatidylcholine Vesicles. *J. Chem. Soc., Perkin Trans. 2* **1993**, 1011−1020.

(7) Pregel, M. J.; Jullien, L.; Canceill, J.; Lacombe, L.; Lehn, J. M. Channel-Type Molecular-Structures 0.4. Transmembrane Transport of

DOI: 10.1021/acsami.6b08620
ACS Appl. Mater. Interfaces 2016, 8, 27987−27995

Alkali-Metal Ions by Bouquet Molecules. *J. Chem. Soc., Perkin Trans. 2* **1995**, 417−426.
(8) Wang, C.; Wang, Z.; Zhang, X. Amphiphilic Building Blocks for Self-Assembly: From Amphiphiles to Supra-amphiphiles. *Acc. Chem. Res.* **2012**, *45*, 608−618.
(9) Liu, K.; Wang, C.; Li, Z.; Zhang, X. Superamphiphiles Based on Directional Charge-Transfer Interactions: From Supramolecular Engineering to Well-Defined Nanostructures. *Angew. Chem., Int. Ed.* **2011**, *50*, 4952−4956.
(10) Wang, G. T.; Wang, C.; Wang, Z. Q.; Zhang, X. H-Shaped Supra-Amphiphiles Based on a Dynamic Covalent Bond. *Langmuir* **2012**, *28*, 14567−14572.
(11) Guo, D.-S.; Wang, K.; Wang, Y.-X.; Liu, Y. Cholinesterase-Responsive Supramolecular Vesicle. *J. Am. Chem. Soc.* **2012**, *134*, 10244−10250.
(12) Samanta, K.; Schmuck, C. Two-component self-assembly of a tetra-guanidiniocarbonyl pyrrole cation and Na(4)EDTA: formation of pH switchable supramolecular networks. *Chem. Commun.* **2015**, *51*, 16065−16067.
(13) Chi, X. D.; Ji, X. F.; Xia, D. Y.; Huang, F. H. A Dual-Responsive Supra-Amphiphilic Polypseudorotaxane Constructed from a Water-Soluble Pillar[7]arene and an Azobenzene-Containing Random Copolymer. *J. Am. Chem. Soc.* **2015**, *137*, 1440−1443.
(14) Yao, Y.; Chi, X. D.; Zhou, Y. J.; Huang, F. H. A bola-type supra-amphiphile constructed from a water-soluble pillar[5]arene and a rod-coil molecule for dual fluorescent sensing. *Chem. Sci.* **2014**, *5*, 2778−2782.
(15) Yu, G. C.; Tang, G. P.; Huang, F. H. Supramolecular enhancement of aggregationinduced emission and its application in cancer cell imaging. *J. Mater. Chem. C* **2014**, *2*, 6609−6617.
(16) Tao, W.; Liu, Y.; Jiang, B. B.; Yu, S. R.; Huang, W.; Zhou, Y. F.; Yan, D. Y. A Linear-Hyperbranched Supramolecular Amphiphile and Its Self-Assembly into Vesicles with Great Ductility. *J. Am. Chem. Soc.* **2012**, *134*, 762−764.
(17) Jiang, L. X.; de Folter, J. W. J.; Huang, J. B.; Philipse, A. P.; Kegel, W. K.; Petukhov, A. V. Helical Colloidal Sphere Structures through Thermo-Reversible Co-Assembly with Molecular Microtubes. *Angew. Chem., Int. Ed.* **2013**, *52*, 3364−3368.
(18) Jiang, L. X.; Yan, Y.; Huang, J. B. Versatility of cyclodextrins in self-assembly systems of amphiphiles. *Adv. Colloid Interface Sci.* **2011**, *169*, 13−25.
(19) Jiang, L. X.; Peng, Y.; Yan, Y.; Huang, J. B. Aqueous self-assembly of SDS@2 beta-CD complexes: lamellae and vesicles. *Soft Matter* **2011**, *7*, 1726−1731.
(20) Jiang, L. X.; Yan, Y.; Huang, J. B. Zwitterionic surfactant/cyclodextrin hydrogel: microtubes and multiple responses. *Soft Matter* **2011**, *7*, 10417−10423.
(21) Yan, Y.; Jiang, L. X.; Huang, J. B. Unveil the potential function of CD in surfactant systems. *Phys. Chem. Chem. Phys.* **2011**, *13*, 9074−9082.
(22) Jiang, L. X.; Peng, Y.; Yan, Y.; Deng, M. L.; Wang, Y. L.; Huang, J. B. "Annular Ring" microtubes formed by SDS@2 beta-CD complexes in aqueous solution. *Soft Matter* **2010**, *6*, 1731−1736.
(23) Luo, J.; Xie, Z.; Lam, J. W. Y.; Cheng, L.; Chen, H.; Qiu, C.; Kwok, H. S.; Zhan, X.; Liu, Y.; Zhu, D.; Tang, B. Z. Aggregation-induced emission of 1-methyl-1,2,3,4,5-pentaphenylsilole. *Chem. Commun.* **2001**, *37*, 1740−1741.
(24) Qin, W.; Yang, Z.; Jiang, Y.; Lam, J. W. Y.; Liang, G.; Kwok, H. S.; Tang, B. Z. Construction of Efficient Deep Blue Aggregation-Induced Emission Luminogen from Triphenylethene for Nondoped Organic Light-Emitting Diodes. *Chem. Mater.* **2015**, *27*, 3892−3901.
(25) Huang, J.; Jiang, Y.; Yang, J.; Tang, R.; Xie, N.; Li, Q.; Kwok, H. S.; Tang, B. Z.; Li, Z. Construction of efficient blue AIE emitters with triphenylamine and TPE moieties for non-doped OLEDs. *J. Mater. Chem. C* **2014**, *2*, 2028−2036.
(26) Yuan, Y.; Kwok, R. T. K.; Tang, B. Z.; Liu, B. Targeted Theranostic Platinum(IV) Prodrug with a Built-In Aggregation-Induced Emission Light-Up Apoptosis Sensor for Noninvasive Early Evaluation of Its Therapeutic Responses in Situ. *J. Am. Chem. Soc.* **2014**, *136*, 2546−2554.
(27) Chan, C. Y. K.; Lam, J. W. Y.; Deng, C.; Chen, X.; Wong, K. S.; Tang, B. Z. Synthesis, Light Emission, Explosive Detection, Fluorescent Photopatterning, and Optical Limiting of Disubstituted Polyacetylenes Carrying Tetraphenylethene Luminogens. *Macromolecules* **2015**, *48*, 1038−1047.
(28) Kwok, R. T. K.; Leung, C. W. T.; Lam, J. W. Y.; Tang, B. Z. Biosensing by luminogens with aggregation-induced emission characteristics. *Chem. Soc. Rev.* **2015**, *44* (13), 4228−4238.
(29) Wang, Z.; Chen, S.; Lam, J. W. Y.; Qin, W.; Kwok, R. T. K.; Xie, N.; Hu, Q.; Tang, B. Z. Long-Term Fluorescent Cellular Tracing by the Aggregates of AIE Bioconjugates. *J. Am. Chem. Soc.* **2013**, *135*, 8238−8245.
(30) Leung, C. W. T.; Hong, Y.; Chen, S.; Zhao, E.; Lam, J. W. Y.; Tang, B. Z. A Photostable AIE Luminogen for Specific Mitochondrial Imaging and Tracking. *J. Am. Chem. Soc.* **2013**, *135*, 62−65.
(31) Ding, D.; Li, K.; Liu, B.; Tang, B. Z. Bioprobes Based on AIE Fluorogens. *Acc. Chem. Res.* **2013**, *46*, 2441−2453.
(32) Qin, W.; Ding, D.; Liu, J.; Yuan, W. Z.; Hu, Y.; Liu, B.; Tang, B. Z. Biocompatible Nanoparticles with Aggregation-Induced Emission Characteristics as Far-Red/Near-Infrared Fluorescent Bioprobes for In Vitro and In Vivo Imaging Applications. *Adv. Funct. Mater.* **2012**, *22*, 771−779.
(33) Xia, Y.; Dong, L.; Jin, Y.; Wang, S.; Yan, L.; Yin, S.; Zhou, S.; Song, B. Water-soluble nano-fluorogens fabricated by self-assembly of bolaamphiphiles bearing AIE moieties: towards application in cell imaging. *J. Mater. Chem. B* **2015**, *3*, 491−497.
(34) Hong, Y.; Lam, J. W. Y.; Tang, B. Z. Aggregation-induced emission. *Chem. Soc. Rev.* **2011**, *40*, 5361−5388.
(35) Mei, J.; Leung, N. L. C.; Kwok, R. T. K.; Lam, J. W. Y.; Tang, B. Z. Aggregation-Induced Emission: Together We Shine, United We Soar! *Chem. Rev.* **2015**, *115*, 11718−11940.
(36) Li, H. K.; Zheng, X. Y.; Su, H. M.; Lam, J. W. Y.; Wong, K. S.; Xue, S.; Huang, X. J.; Huang, X. H.; Li, B. S.; Tang, B. Z. Synthesis, optical properties, and helical self-assembly of a bivaline-containing tetraphenylethene. *Sci. Rep.* **2016**, *6*, 19277.
(37) Li, H. K.; Cheng, J.; Deng, H. Q.; Zhao, E. G.; Shen, B.; Lam, J. W. Y.; Wong, K. S.; Wu, H. K.; Li, B. S.; Tang, B. Z. Aggregation-induced chirality, circularly polarized luminescence, and helical self-assembly of a leucine-containing AIE luminogen. *J. Mater. Chem. C* **2015**, *3*, 2399−2404.
(38) Li, H. K.; Cheng, J.; Zhao, Y. H.; Lam, J. W. Y.; Wong, K. S.; Wu, H. K.; Li, B. S.; Tang, B. Z. L-Valine methyl ester-containing tetraphenylethene: aggregation-induced emission, aggregation-induced circular dichroism, circularly polarized luminescence, and helical self-assembly. *Mater. Horiz.* **2014**, *1*, 518−521.
(39) Yuan, W. Z.; Mahtab, F.; Gong, Y. Y.; Yu, Z. Q.; Lu, P.; Tang, Y. H.; Lam, J. W. Y.; Zhu, C. Z.; Tang, B. Z. Synthesis and self-assembly of tetraphenylethene and biphenyl based AIE- active triazoles. *J. Mater. Chem.* **2012**, *22*, 10472−10479.
(40) Chan, K. H. Y.; Lam, J. W. Y.; Wong, K. M. C.; Tang, B. Z.; Wing-Wah Yam, V. Chiral Poly(4-ethynylbenzoyl-L-valine)-Induced Helical Self-Assembly of Alkynylplatinum(II) Terpyridyl Complexes with Tunable Electronic Absorption, Emission, and Circular Dichroism Changes. *Chem. - Eur. J.* **2009**, *15*, 2328−2334.
(41) Zhang, M.; Yin, X. P.; Tian, T.; Liang, Y.; Li, W. N.; Lan, Y.; Li, J.; Zhou, M. M.; Ju, Y.; Li, G. T. AIE-induced fluorescent vesicles containing amphiphilic binding pockets and the FRET triggered by host-guest chemistry. *Chem. Commun.* **2015**, *51*, 10210−10213.
(42) Dakwar, G. R.; Hammad, I. A.; Popov, M.; Linder, C.; Grinberg, S.; Heldman, E.; Stepensky, D. Delivery of proteins to the brain by bolaamphiphilic nano-sized vesicles. *J. Controlled Release* **2012**, *160*, 315−321.
(43) Zelzer, M.; Todd, S. J.; Hirst, A. R.; McDonald, T. O.; Ulijn, R. V. Enzyme responsive materials: design strategies and future developments. *Biomater. Sci.* **2013**, *1*, 11−39.

DOI: 10.1021/acsami.6b08620
ACS Appl. Mater. Interfaces 2016, 8, 27987−27995

(44) Ding, Y.; Kang, Y.; Zhang, X. Enzyme-responsive polymer assemblies constructed through covalent synthesis and supramolecular strategy. *Chem. Commun.* **2015**, *51*, 996−1003.
(45) Jiang, L.; Yan, Y.; Drechsler, M.; Huang, J. Enzyme-triggered model self-assembly in surfactant-cyclodextrin systems. *Chem. Commun.* **2012**, *48*, 7347−7349.
(46) Hu, J.; Zhang, G.; Liu, S. Enzyme-responsive polymeric assemblies, nanoparticles and hydrogels. *Chem. Soc. Rev.* **2012**, *41*, 5933−5949.
(47) Yang, Z. Y.; Qin, W.; Leung, N. L. C.; Arseneault, M.; Lam, J. W. Y.; Liang, G. D.; Sung, H. H. Y.; Williams, I. D.; Tang, B. Z. A mechanistic study of AIE processes of TPE luminogens: intramolecular rotation vs. configurational isomerization. *J. Mater. Chem. C* **2016**, *4*, 99−107.
(48) Zhao, Z. J.; Chan, C. Y. K.; Chen, S. M.; Deng, C. M.; Lam, J. W. Y.; Jim, C. K. W.; Hong, Y. N.; Lu, P.; Chang, Z. F.; Chen, X. P.; Lu, P.; Kwok, H. S.; Qiu, H. Y.; Tang, B. Z. Using tetraphenylethene and carbazole to create efficient luminophores with aggregation-induced emission, high thermal stability, and good hole-transporting property. *J. Mater. Chem.* **2012**, *22*, 4527−4534.
(49) Zhao, N.; Li, M.; Yan, Y. L.; Lam, J. W. Y.; Zhang, Y. L.; Zhao, Y. S.; Wong, K. S.; Tang, B. Z. A tetraphenylethene-substituted pyridinium salt with multiple functionalities: synthesis, stimuli-responsive emission, optical waveguide and specific mitochondrion imaging. *J. Mater. Chem. C* **2013**, *1*, 4640−4646.
(50) Shi, H. P.; Gong, Z. H.; Xin, D. H.; Roose, J.; Peng, H. R.; Chen, S. M.; Lam, J. W. Y.; Tang, B. Z. Synthesis, aggregation-induced emission and electroluminescence properties of a novel compound containing tetraphenylethene, carbazole and dimesitylboron moieties. *J. Mater. Chem. C* **2015**, *3*, 9095−9102.
(51) Zhao, L.; Jiang, L. X.; Han, Y. C.; Xian, Z. Y.; Huang, J. B.; Yan, Y. A case of cyclodextrin-catalyzed self-assembly of an amphiphile into microspheres. *Soft Matter* **2013**, *9*, 7710−7717.
(52) Forbes, C. C.; DiVittorio, K. M.; Smith, B. D. Bolaamphiphiles Promote Phospholipid Translocation Across Vesicle Membranes. *J. Am. Chem. Soc.* **2006**, *128* (28), 9211−9218.
(53) Yan, Y.; Xiong, W.; Huang, J.; Li, Z.; Li, X.; Li, N.; Fu, H. Organized Assemblies in Bolaamphiphile/Oppositely Charged Conventional Surfactant Mixed Systems. *J. Phys. Chem. B* **2005**, *109*, 357−364.
(54) Chen, Z.-X.; Su, X.-X.; Deng, S.-P. Molecular Recognition of Melamine by Vesicles Spontaneously Formed from Orotic Acid Derived Bolaamphiphiles. *J. Phys. Chem. B* **2011**, *115*, 1798−1806.
(55) Yan, Y.; Huang, J.; Li, Z.; Ma, J.; Fu, H.; Ye, J. Vesicles with Superior Stability at High Temperature. *J. Phys. Chem. B* **2003**, *107*, 1479−1482.
(56) Jiang, L.; Peng, Y.; Yan, Y.; Huang, J. Aqueous self-assembly of SDS@2[small beta]-CD complexes: lamellae and vesicles. *Soft Matter* **2011**, *7*, 1726−1731.
(57) Whitehouse, P.; Price, D.; Struble, R.; Clark, A.; Coyle, J.; Delon, M. Alzheimer's disease and senile dementia: loss of neurons in the basal forebrain. *Science* **1982**, *215*, 1237−1239.
(58) Selkoe, D. J. Alzheimer's Disease: Genes, Proteins, and Therapy. *Physiol. Rev.* **2001**, *81*, 741−766.

DOI: 10.1021/acsami.6b08620
ACS Appl. Mater. Interfaces 2016, 8, 27987−27995